

Supplementary Materials

Mechanical hydrolysis imparts self-destruction of water molecules under steric confinement

Ehsan Hosseini¹, Mohammad Zakertabrizi¹, Asghar Habibnejad Korayem^{1,2*}, Paola Carbone³, Ali Esfandiar^{4*}, and Rouzbeh Shahsavari^{5*}

¹Nanomaterials Research Centre, School of Civil Engineering, Iran University of Science and Technology, Tehran, Iran

²Department of Civil Engineering, Monash University, Clayton, Victoria, Australia

³School of Chemical Engineering and Analytical Science, University of Manchester, Oxford Road, Manchester, M13 9PL, United Kingdom

⁴Department of Physics, Sharif University of Technology, Tehran 11155-9161, Iran

⁵Department of Civil and Environmental Engineering, Rice University, Houston, Texas 77005, United States

Table of Contents

Supplementary Descriptions	3
Supplementary Figures	6
Supplementary References	17

Supplementary Descriptions

Figure S1 shows the details of the simulation cell used for DFT calculations. Figure S1a-b show one and 20 water molecules between two graphene sheets, respectively. The external pressure is applied with another graphene sheet as a mediator, to better distribute the pressure across the lower nanosheet.

Figure S2 depicts the process of applying pressure on the original water droplet (Figure S2a). Figure S2b shows the final steps of the process, where the droplet is completely spread to a single layer.

Figure S3 shows the Radial distribution Function (RDF) values for O-O pairs inside the confinement for two different interlayer distance values. In the main manuscript, we discuss the breaking down of the ice-like formation after the significant orbital overlap enforced by severe confinement. From 5.4 to 3.4 Å, where the graphene-water interaction changes from vdW pressure to full orbital overlap, distance between the water molecules experiences a slight increase. We have interpreted this as the elongation or elimination of some of the hydrogen bonds and divergence of some water molecules from their initial quadrilateral formation.

Figure S4a shows the arrangement of water molecules inside two graphene layers with 4.4 Å interlayer space in between. The predominance of van der Waals interaction is depicted here, with water molecules forming in square formation (Figure S4b), linked by hydrogen bond. This is where the structure starts to fall apart due to the increasing orbital overlap of the water molecules and graphene.

Figure S5 shows the process of functionalization in three steps, with more details about the positioning of the concerning molecules. In the normal conditions, where van der Waals forces

are predominant, if the interlayer distance is reduced to 4.4 Å the water molecules try to preserve an ice-like formation (with the O-H bond axes being parallel to the graphene plane) under high van der Waals pressure as shown in Figure S5a. Reducing the distance to 3.4 Å, the extreme confinement drives the water molecules into a closer interaction with the closest carbon atom, where the O-H axis forms a 103°-109° angle with the O-C axis as shown in Figure S5b. This angle increases to 109°, here shown in Figure S5c, where it coincides with the release of the other hydrogen as proton in the interlayer space.

Figure S6 shows the formation process of epoxy, as the less common functional group formed after hydrolysis. At 3.4 Å interlayer distance, which is the original interlayer distance for graphene, water molecules are hard pressed to keep a parallel stance (with regards to the O-H bond axes and the graphene baseline) at first, shown in Figure S6a. The transferred charge and the forced overlap of the orbitals, in the process that was mentioned in the main script, causes the formation of a hydroxyl group while releasing a proton. The problem is that the actual length of the C-OH bond is 1.8 Å, which means the distance between the oxygen atom and the other graphene layers to 1.6 Å, as shown in Figure S6b. The pressure forces the oxygen to lose another hydrogen, forming a bond with one of the adjunct carbon atoms and creating of epoxy functional group, here shown in Figure S6c.

Figure S7 shows the C-C bond length distribution for the carbon atoms in functionalized graphene. As a result of functionalization, carbon atoms change from sp^2 to sp^3 hybridization. Bond length provide a good representation of this phenomenon, as the share of longer bonds increases with the increase in the number of functional groups.

Figure S8 shows the bandgap structure for the bilayer graphene (with and without confined water) with two different interlayer distance values (3.4 and 4.4 Å). These figures present more

evidence of the integration. Comparing the bandgap structure of the graphene nanosheets with confined water molecules against their dry counterparts with 3.4 Å interlayer spacing (Figure S8a), show a reduction in the energy gaps, with the bandgap standing at 0.6 eV. The 4.4 Å model, shown in Figure S8b, on the other hand, demonstrates a wider band structure with higher bandgap at 1.4 eV. Albeit both structures show similar bandgap structure when no water is involved, their behavior is quite different when water exists in the interlayer region.

Figure S9 shows the graphite interlayer distance versus the external physical pressure it needs to be achieved. The natural interlayer distance of graphene sheets is 3.4 Å. Applying an external force around 40 GPa, decreases the interlayer distance to 2.688 Å. Increasing the external force to 80 GPa forces the graphene sheets to an even lower distance (2.335 Å), without covalent interaction. This shows that graphene sheets cannot bond under much larger physical pressure compared with the physical pressure needed for induced hydrolysis.

Figure S10 shows the stress-strain curve of the GO (functionalized through hydrolysis) obtained through DFT calculations. Both functionals show approximately the same ultimate stress for the produced GO (one-side functionalized), which is around 65 GPa.

Figure S11 shows the same curve as Figure S10, but obtained by through MD simulations. The ultimate stress is around 60 GPa for the one-side functionalized GO. This value is around 50 GPa for the two-side functionalized GO.

Another slight difference between results is the difference in the ultimate strain. For the model analyzed by DFT this value is 0.17, which is lower than the results from MD analysis at 0.2.

In general, the distance between consecutive oxygen atoms, which act as hopping stations for protons, is the major factor that determines the facility of the flow. Although this barrier is a

function of a variety of parameters (more information provided in the supplementary file), it is selected as an index for comparing different patterns of functionalization and the average distance between oxygen atoms in different environments in Figure S12a.

Although the energy barrier in water is shown to be the lowest, the difference is not great enough to halt the flow of protons when passing from one environment to the other, assuming the distance between the oxygen atoms remains the same. As this distance decreases, the energy difference fades, reaching near zero at 2.4 Å. This idea is strengthened with the data shown in Figure S12b, where the jumping tendency of protons is measured in terms of bonding energy between one proton and its immediate oxygen against the distance between the neighboring oxygen atoms. Here, the interval between 2.3 to 2.4 Å shows the lowest amount of resistance, which corresponds with the apex in jumping tendency; this interval also coincides with the lowest amounts of the energy barrier, as depicted in Figure S12a. Consequently, the hydroxyl groups spaced 2.4 Å from each other are best suited to facilitate and preserve the proton flow, as the attraction is maximum and the barrier is reasonably low. This is the optimal spacing, where the attraction is enough to attract incoming protons, but not enough to completely capture them. On the other hand, the repulsion is enough to help them hop to the next station, but not enough to halt the proton flow.

Supplementary Figures

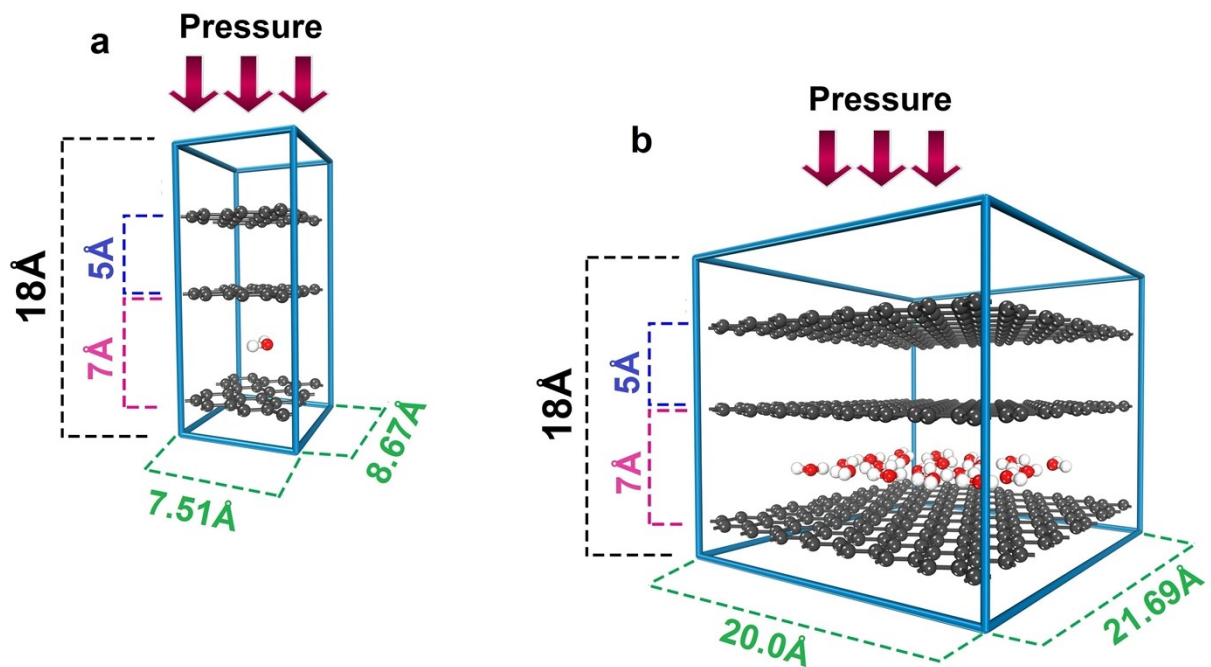


Figure S1. The pattern of models DFT, shown in the original design: (a) one water molecule restrained between two $7.51 \times 8.67 \text{ \AA}$ graphene sheets, and (b) 20 water molecules restrained between two $20.0 \times 21.69 \text{ \AA}$ graphene sheets.

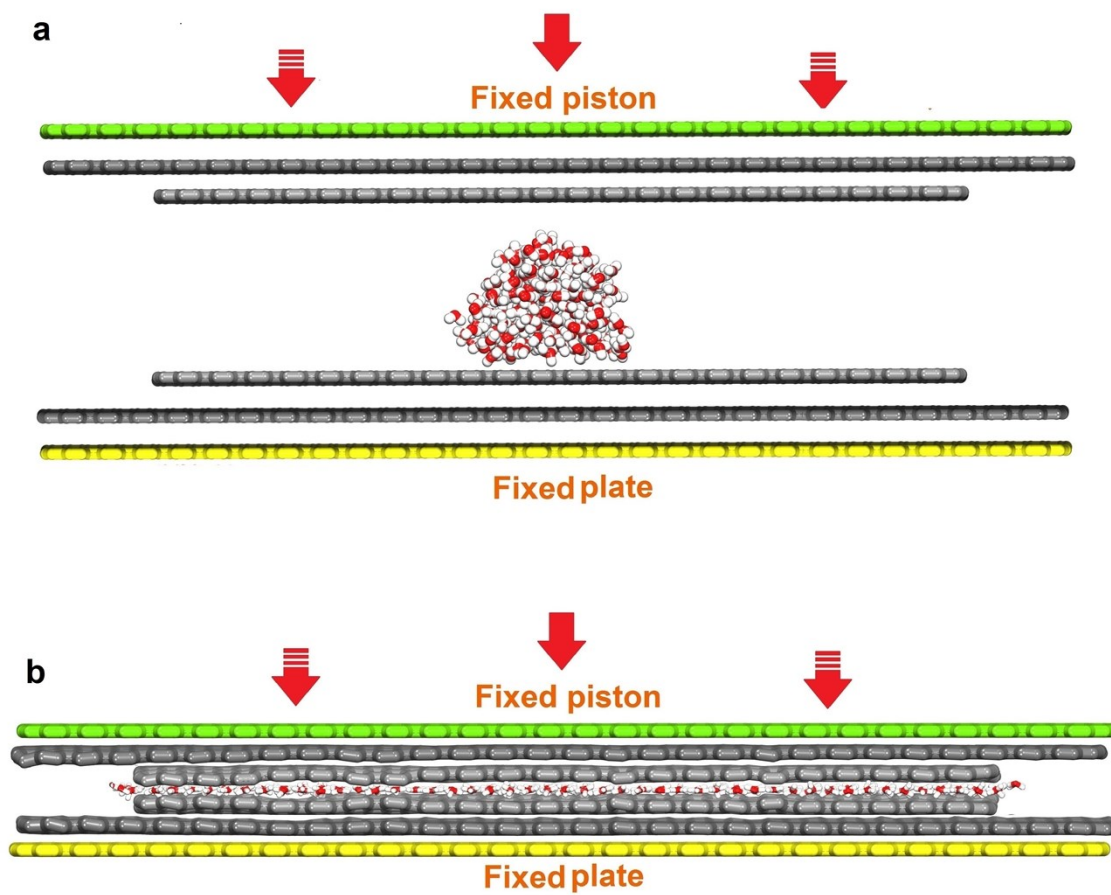


Figure S2. The process of decreasing the interlayer distance to the desired value, shown in the original design of the model: (a) drop of water confined between the moving upper platelet and the fixed platelet, and (b) water confined between the graphene membranes, both fixed.

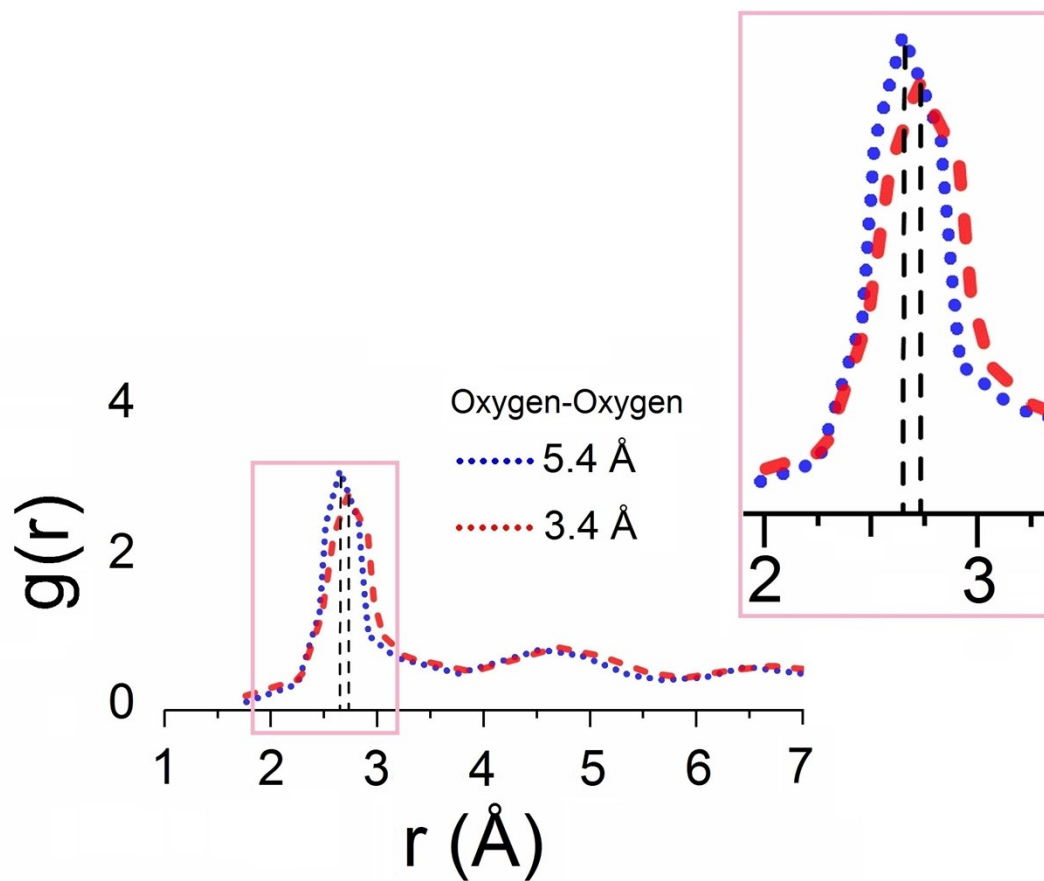


Figure S3. RDF values for the oxygen atoms of water in the interlayer space of 5.4 and 3.4 \AA between two graphene sheets.

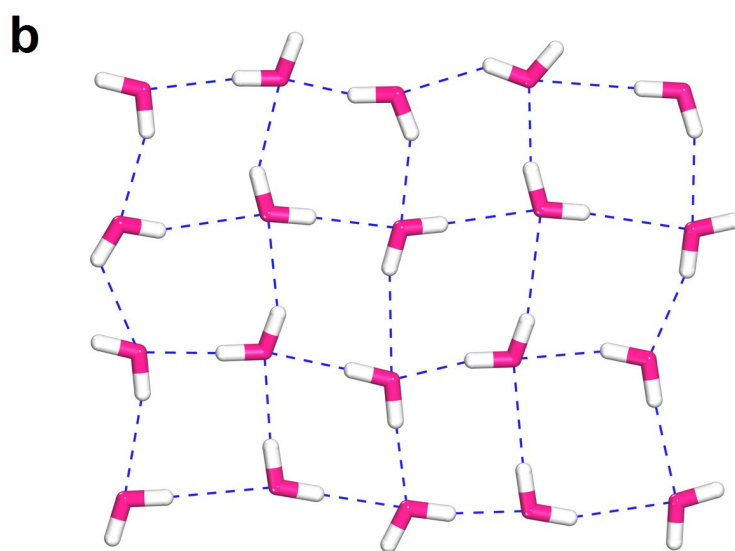
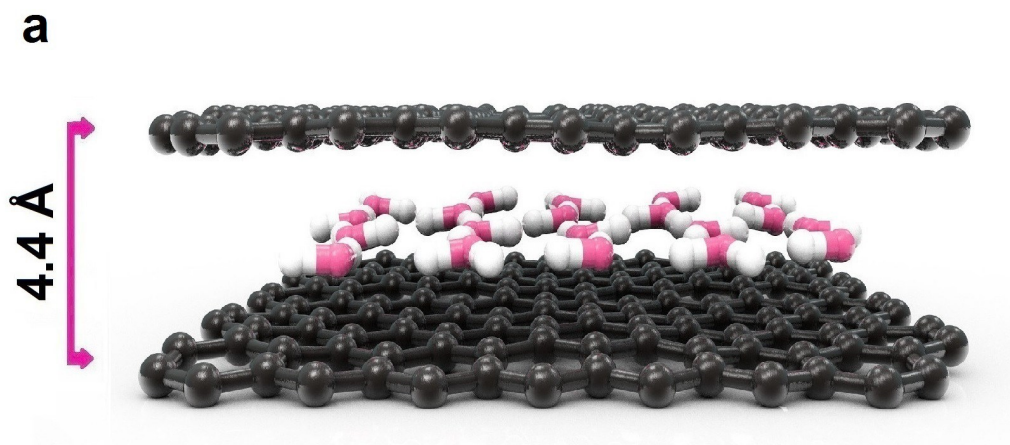


Figure S4. (a) Water molecules confined in between graphene nanosheets spaced at 4.4 Å. square formation and (b) hydrogen bonds between the water molecules create quadrilateral ice crystals

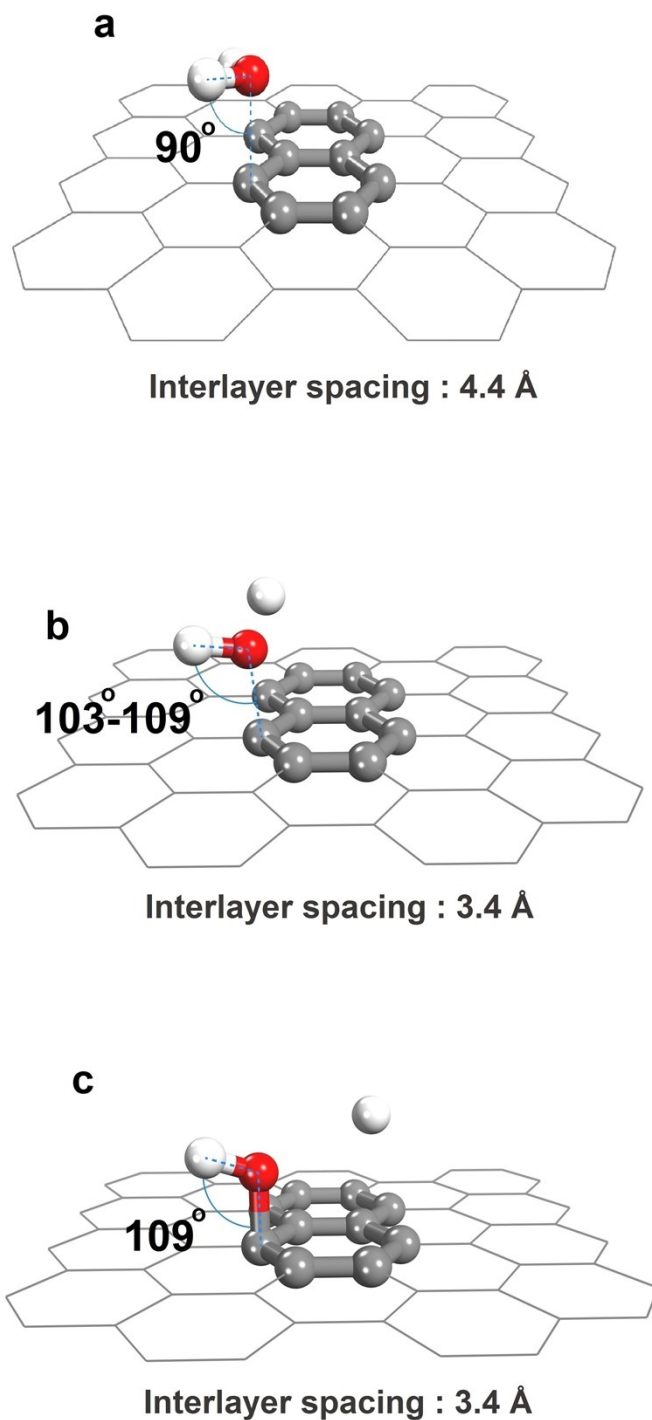


Figure S5. Water molecule relative positioning towards the graphene sheet: (a) O-H bonds are parallel with the graphene sheet in 4.4 Å interlayer, (b) the initial stance of water molecule in the 3.4 Å interlayer, which then transforms into (c) functionalization of the graphene membrane and the release of proton

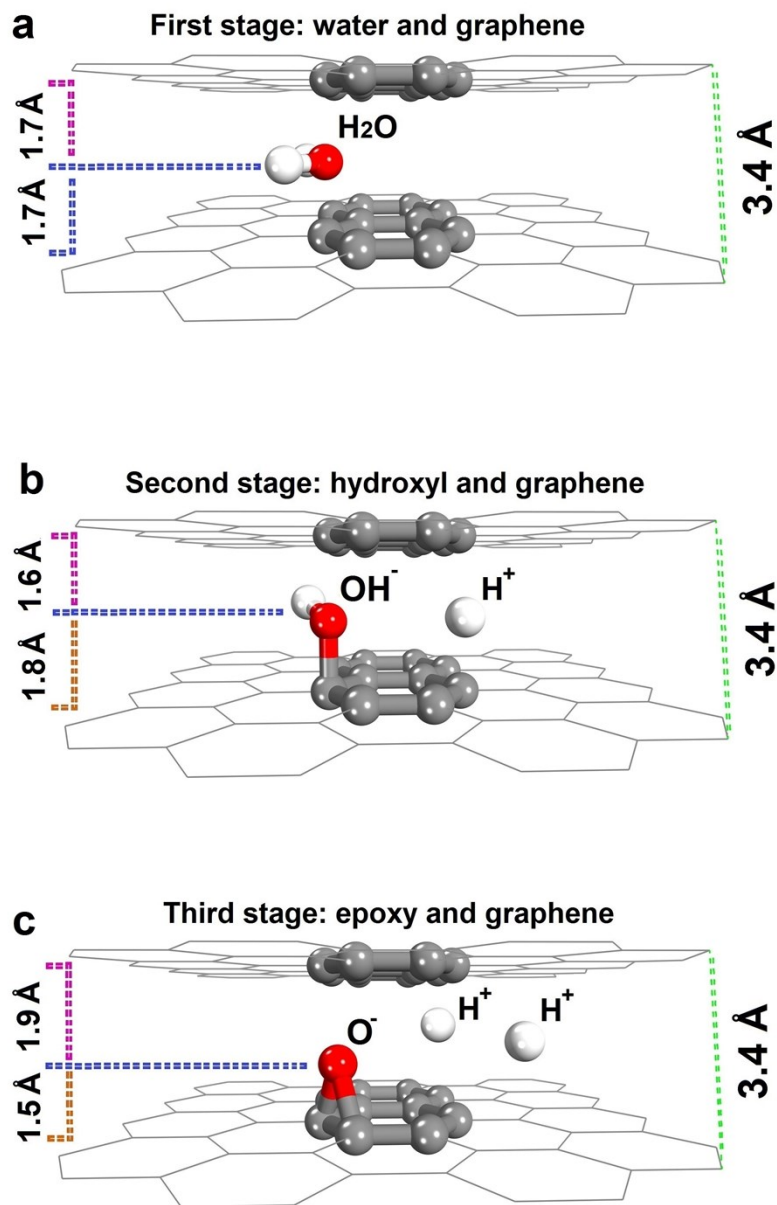


Figure S6. Formation of epoxy functional group: (a) water confined in 3.4 Å interlayer space, (b) losing the first proton, formation of hydroxyl group, and (c) losing the second proton, formation of epoxy group

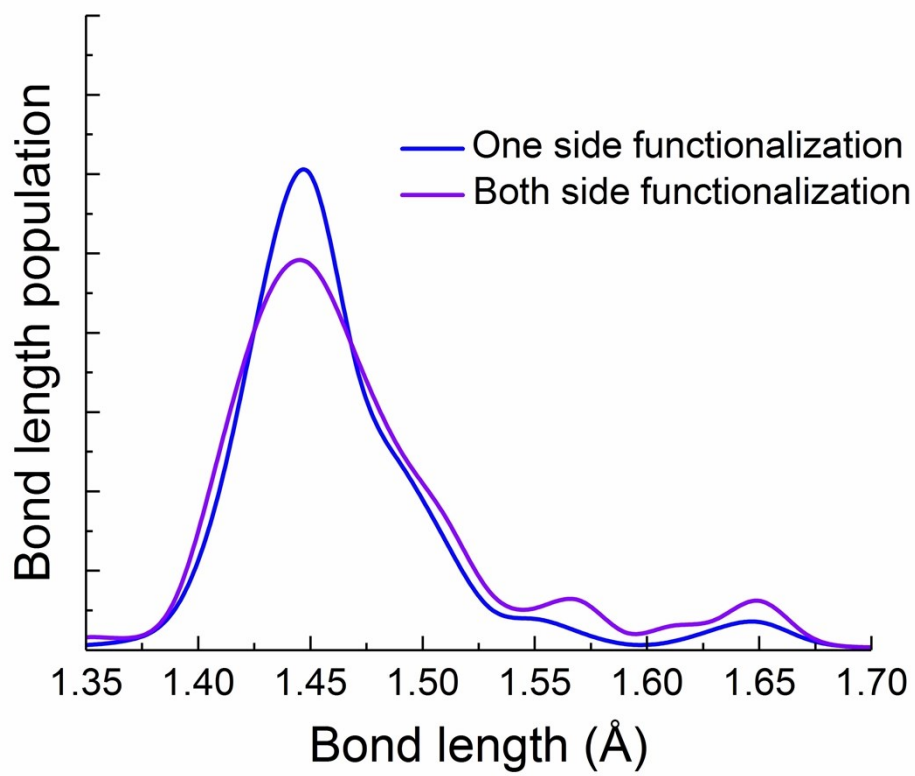


Figure S7. Carbon-carbon bond length distribution for the functionalized graphene through hydrolysis.

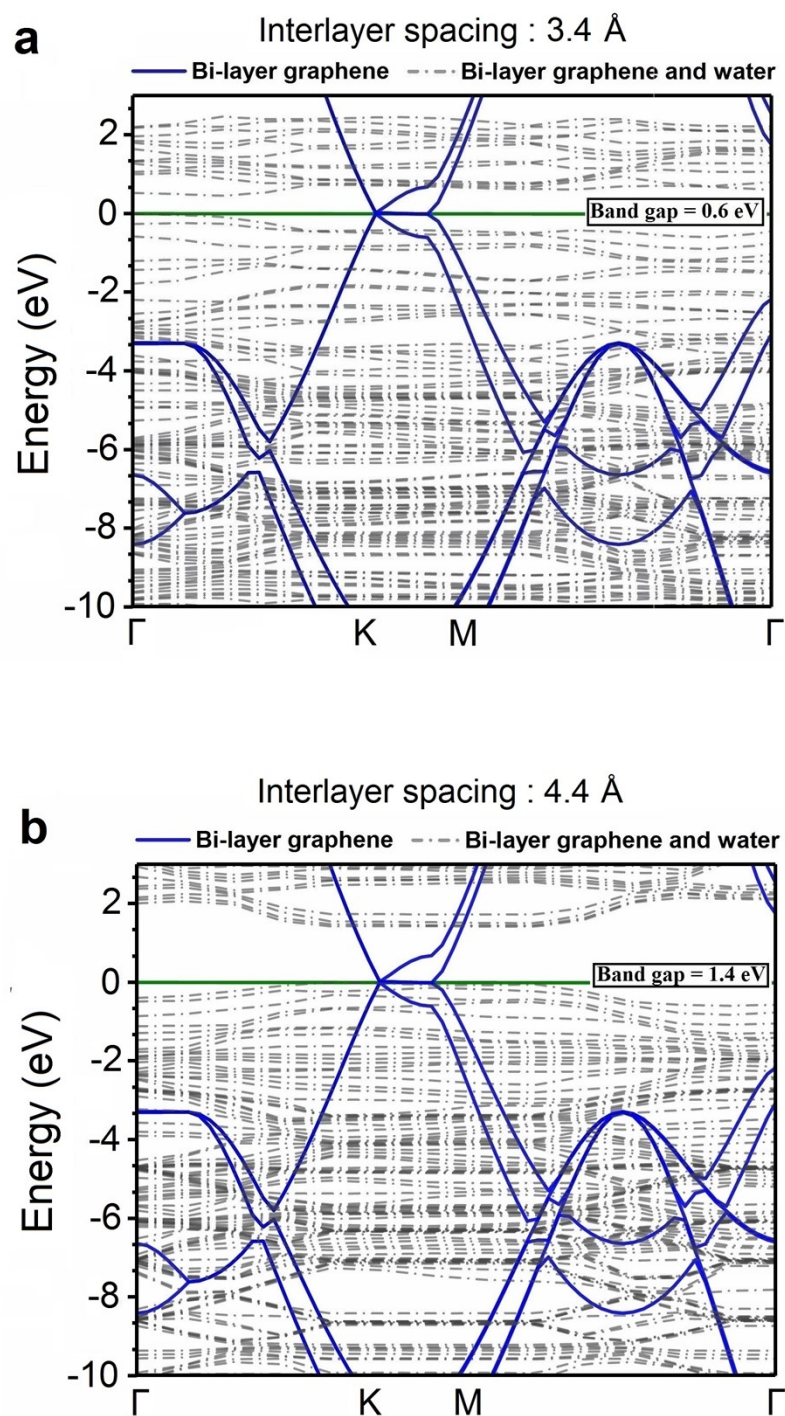


Figure S8. The bandgap structure of bilayer graphene, at the background, and the bilayer-water model with the interlayer spacing of (a) 3.4 Å and (b) 4.4 Å

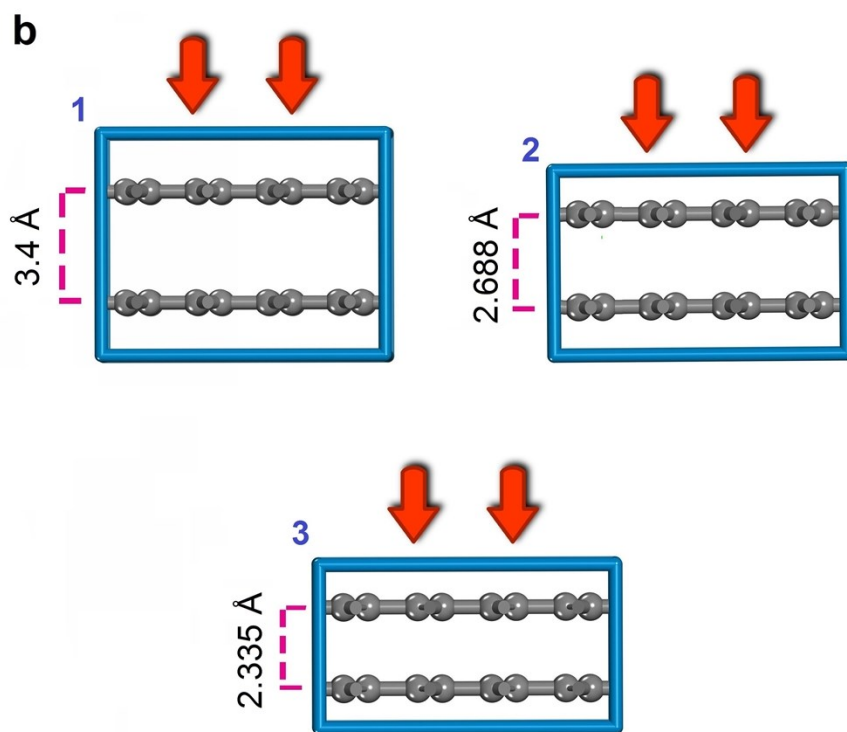
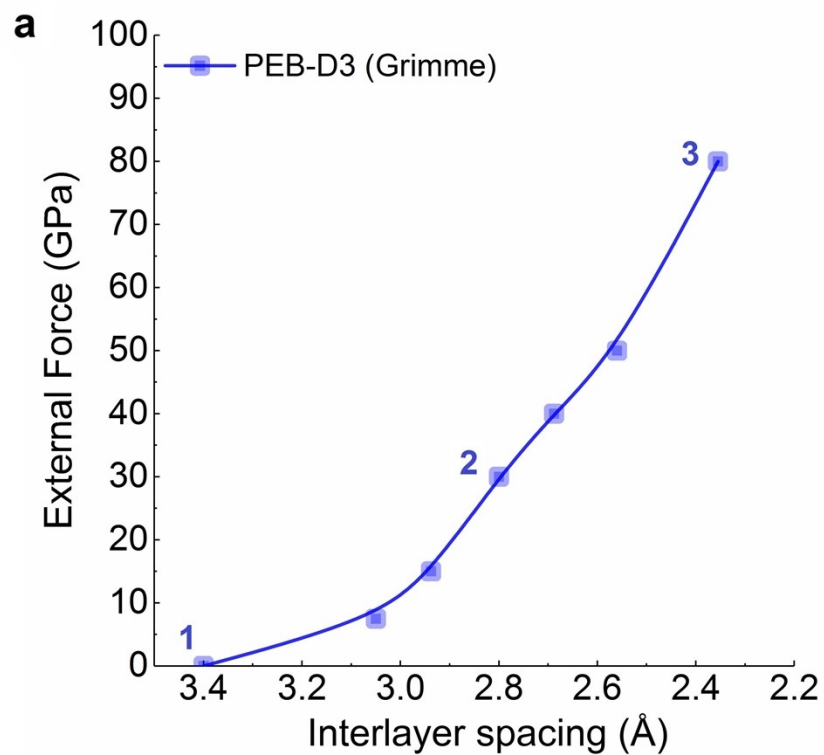


Figure S9. Effect of external force on the interlayer distance of graphene sheets

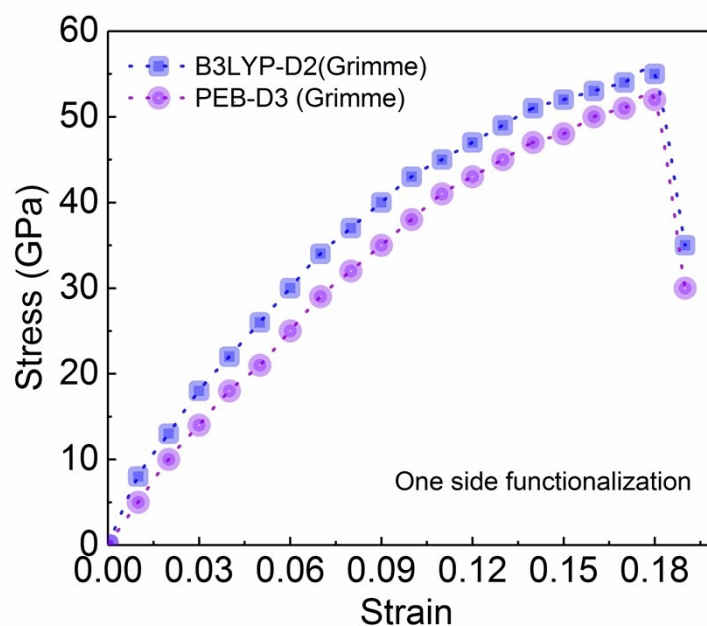


Figure S10. Stress-strain curve for GO, functionalized through hydrolysis, obtained with DFT calculations through two different functionals

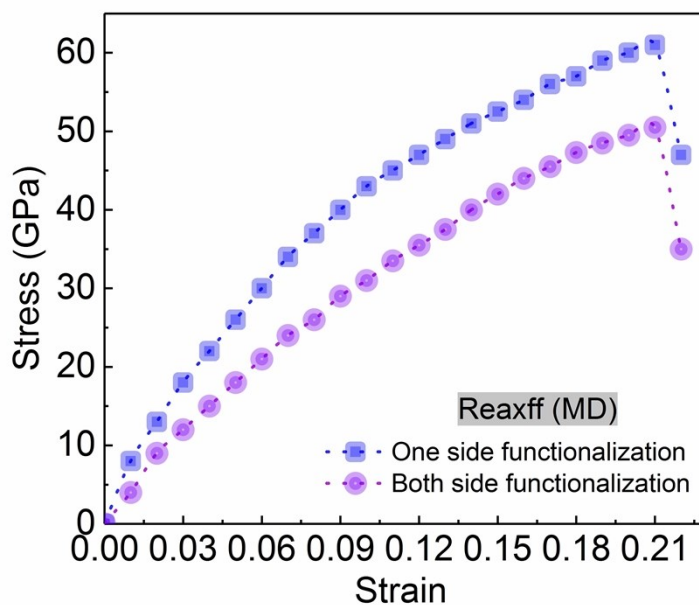


Figure S11. Stress-strain curve of the GO, functionalized through hydrolysis, obtained with MD simulations in REAXX-FF

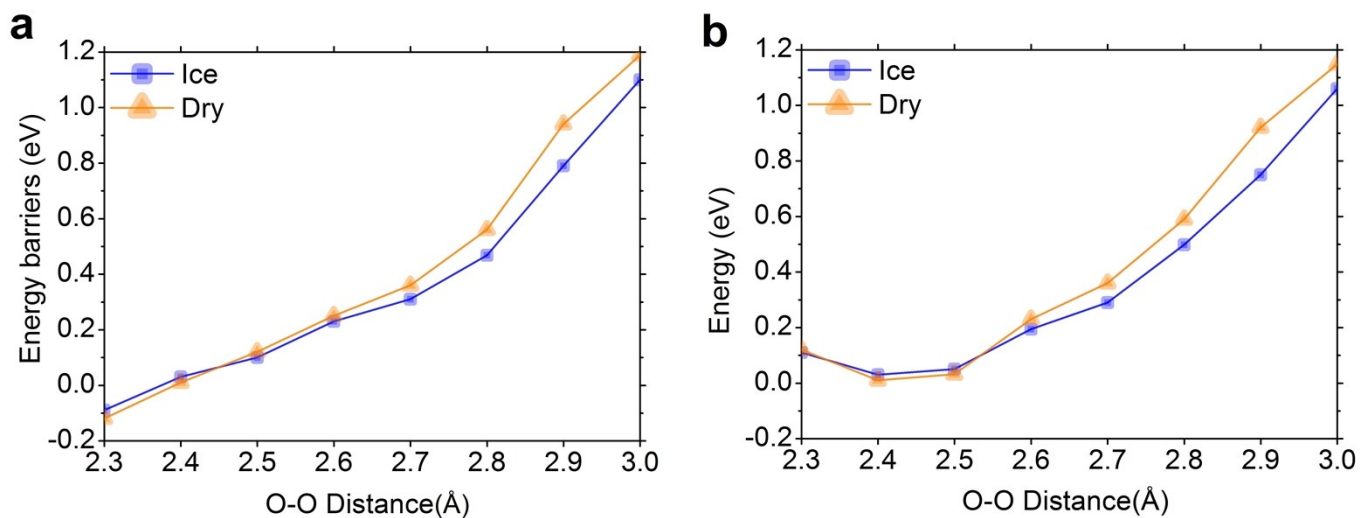


Figure S12. (a) The energy barrier and the (b) hopping tendency of protons (represented by the bonding energy between hydrogen atoms of hydronium and the oxygen atom in their immediate neighborhood) is also depicted against the average distance between oxygen atoms, used as hoping points for the protons in REAXX-FF